

Model independent constraints on clustering and growth of cosmic structures from intensity mapping

Alessio Suriano

Stefano Camera

Isabella Paola Carucci

Centro de Astrofísica da Universidade do Porto

May 23, 2022



Table of Contents

Introduction

Template fitting

Intensity mapping

Analysis

Cosmic structures

$$\delta(\mathbf{r}) = \frac{\rho(\mathbf{r}) - \bar{\rho}}{\bar{\rho}}; \quad \delta(t) = D(t)\delta_i$$

Cosmic structures

$$\delta(\mathbf{r}) = \frac{\rho(\mathbf{r}) - \bar{\rho}}{\bar{\rho}}; \quad \delta(t) = D(t)\delta_i$$

- ▶ Gaussian distribution

$$\langle \delta(\mathbf{r})\delta(\mathbf{r}') \rangle \equiv \xi(|\mathbf{r} - \mathbf{r}'|)$$

Cosmic structures

$$\delta(\mathbf{r}) = \frac{\rho(\mathbf{r}) - \bar{\rho}}{\bar{\rho}}; \quad \delta(t) = D(t)\delta_i$$

- ▶ Gaussian distribution

$$\langle \delta(\mathbf{r})\delta(\mathbf{r}') \rangle \equiv \xi(|\mathbf{r} - \mathbf{r}'|)$$

- ▶ Power spectrum

$$\langle \delta(\mathbf{k})\delta(\mathbf{k}') \rangle = (2\pi)^3 \delta_D^3(\mathbf{k} - \mathbf{k}') P_{\delta\delta}(k)$$

Cosmic structures

$$\delta(\mathbf{r}) = \frac{\rho(\mathbf{r}) - \bar{\rho}}{\bar{\rho}}; \quad \delta(t) = D(t)\delta;$$

- ▶ Gaussian distribution

$$\langle \delta(\mathbf{r})\delta(\mathbf{r}') \rangle \equiv \xi(|\mathbf{r} - \mathbf{r}'|)$$

- ▶ Power spectrum

$$\langle \delta(\mathbf{k})\delta(\mathbf{k}') \rangle = (2\pi)^3 \delta_D^3(\mathbf{k} - \mathbf{k}') P_{\delta\delta}(k)$$

- ▶ Projecting onto a sphere

$$\Delta(\mathbf{r}) = \sum_{lm} a_{lm}(z) Y_{lm}(\hat{\mathbf{r}})$$

$$\langle \Delta(\mathbf{r})\Delta^*(\mathbf{r}') \rangle = \sum_{l=0}^{\infty} C_l \sum_{m=-l}^l Y_{lm}(\hat{\mathbf{r}}) Y_{lm}^*(\hat{\mathbf{r}}')$$

- ▶ physical form of the perturbation variable [1]

$$\Delta(\mathbf{r}) = b(z)\delta(\hat{\mathbf{r}}) + \frac{1}{\mathcal{H}(z)}\partial_r(\mathbf{V}(\mathbf{r}) \cdot \hat{\mathbf{r}}) + \dots$$

- ▶ physical form of the perturbation variable [1]

$$\Delta(\mathbf{r}) = b(z)\delta(\hat{\mathbf{r}}) + \frac{1}{\mathcal{H}(z)}\partial_r(\mathbf{V}(\mathbf{r}) \cdot \hat{\mathbf{r}}) + \dots$$

- ▶ Power spectrum

$$P_{\Delta\Delta}(k, \mu, z) \simeq [b(z)\sigma_8 + f(z)\sigma_8\mu^2]^2 D^2(z) \frac{P_{lin}(k)}{\sigma_8}. \quad (1)$$

- ▶ physical form of the perturbation variable [1]

$$\Delta(\mathbf{r}) = b(z)\delta(\hat{\mathbf{r}}) + \frac{1}{\mathcal{H}(z)}\partial_r(\mathbf{V}(\mathbf{r}) \cdot \hat{\mathbf{r}}) + \dots$$

- ▶ Power spectrum

$$P_{\Delta\Delta}(k, \mu, z) \simeq [b(z)\sigma_8 + f(z)\sigma_8\mu^2]^2 D^2(z) \frac{P_{lin}(k)}{\sigma_8}. \quad (1)$$

- ▶ Harmonic power spectrum

$$C_{ij,\ell}^{gg} = b\sigma_8^i b\sigma_8^j C_{ij,\ell}^{\delta\delta} + f\sigma_8^i f\sigma_8^j C_{ij,\ell}^{VV} + 2b\sigma_8^{(i} f\sigma_8^{j)} C_{ij,\ell}^{\delta V}$$

$$b\sigma_8(z) := b(z)D(z)\sigma_8; \quad f\sigma_8(z) := -\frac{d \ln D(z)}{d \ln(1+z)} D(z)\sigma_8$$

21cm HI emission line

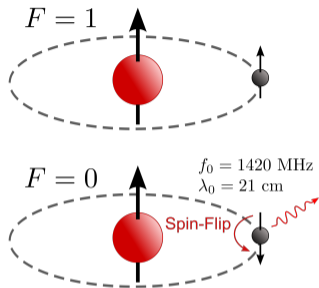


Figure: HI 21cm spin-flip transition between hyperfine states

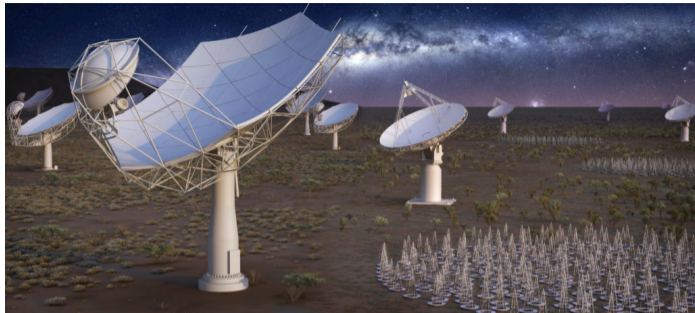


Figure: Square Kilometer Array

$$\frac{dL}{d\Omega d\nu} \propto N_H$$

After reionization HI survives only in **high density regions**.



Good DM halos tracer.

Intensity mapping

Integrating over large volume elements

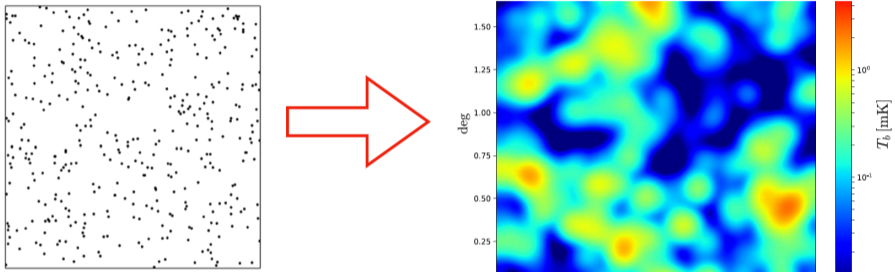


Figure: Galaxies become a temperature map

- ▶ **time-effective**
- ▶ **excellent redshift resolution**

- ▶ **astrophysical foregrounds**
- ▶ **instrumental systematics**

IM simulation

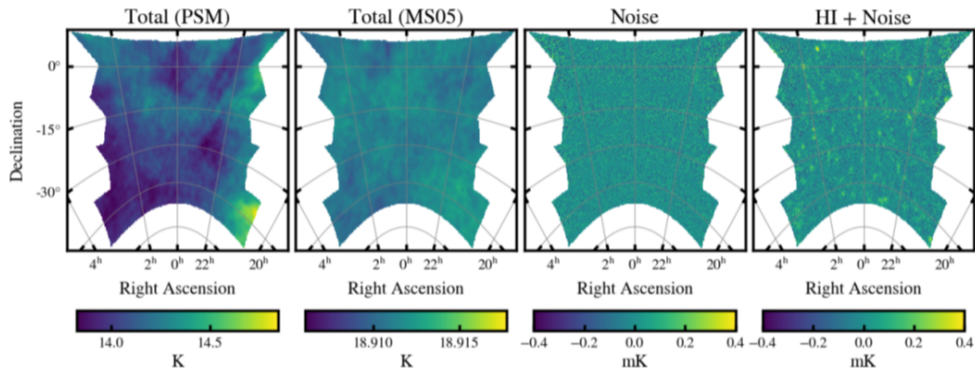


Figure: Maps of the contributing components to the final simulation

Binning the simulation

Top hat(s) functions

$$w_{HI}^i(z) = \frac{1}{2} \left[1 - \tanh \left(\frac{2|z - \bar{z}_i| - \Delta z_i}{\sigma \Delta z_i} \right) \right]$$

$$\sigma = 0.01$$

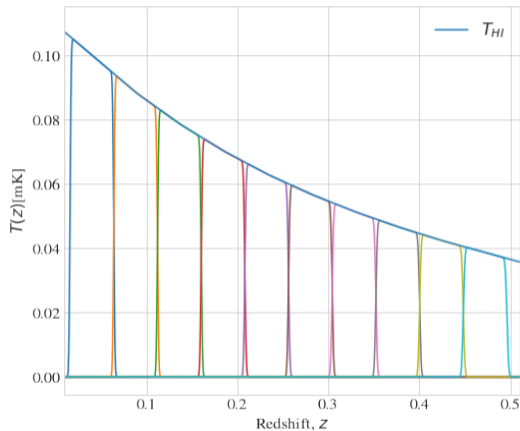
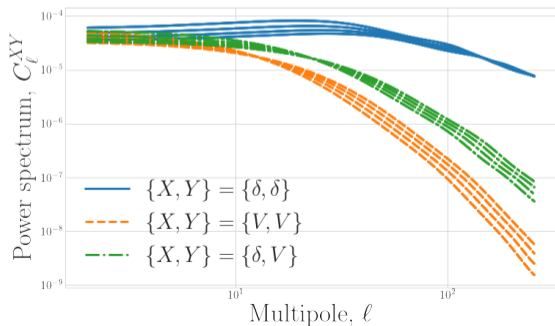
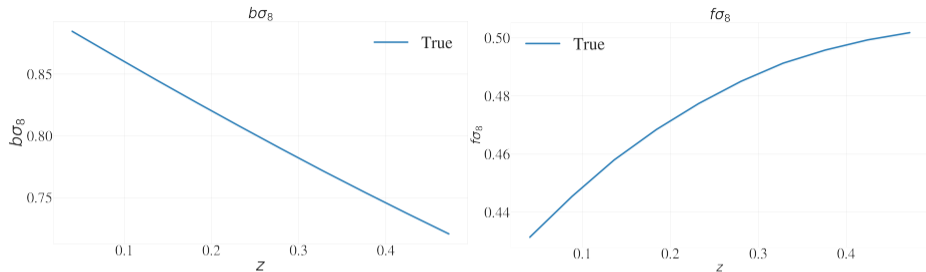


Figure: Bins description

CAMB - Theoretical predictions for cosmological observables



Template fitting

- ▶ Likelihood

$$\ln L(\boldsymbol{\theta}; \mathbf{d}) \propto [\mathbf{d} - \mathbf{m}(\boldsymbol{\theta})]^\top \boldsymbol{\Sigma}^{-1} [\mathbf{d} - \mathbf{m}(\boldsymbol{\theta})]$$

Template fitting

► Likelihood

$$\ln L(\boldsymbol{\theta}; \mathbf{d}) \propto [\mathbf{d} - \mathbf{m}(\boldsymbol{\theta})]^\top \boldsymbol{\Sigma}^{-1} [\mathbf{d} - \mathbf{m}(\boldsymbol{\theta})]$$

► Model

$$m_\ell^{ij}(\boldsymbol{\theta}) = b\sigma_8^i b\sigma_8^j C_{ij,\ell}^{\delta\delta} + f\sigma_8^i f\sigma_8^j C_{ij,\ell}^{VV} + b\sigma_8^i f\sigma_8^j C_{ij,\ell}^{\delta V} + b\sigma_8^j f\sigma_8^i C_{ji,\ell}^{\delta V}$$

Template fitting

► Likelihood

$$\ln L(\boldsymbol{\theta}; \mathbf{d}) \propto [\mathbf{d} - \mathbf{m}(\boldsymbol{\theta})]^\top \boldsymbol{\Sigma}^{-1} [\mathbf{d} - \mathbf{m}(\boldsymbol{\theta})]$$

► Model

$$m_\ell^{ij}(\boldsymbol{\theta}) = b\sigma_8^i b\sigma_8^j C_{ij,\ell}^{\delta\delta} + f\sigma_8^i f\sigma_8^j C_{ij,\ell}^{VV} + b\sigma_8^i f\sigma_8^j C_{ij,\ell}^{\delta V} + b\sigma_8^j f\sigma_8^i C_{ji,\ell}^{\delta V}$$

► Parameters

$$\boldsymbol{\theta} = \{b\sigma_8^i\} \cup \{f\sigma_8^i\}$$

Template fitting

- ▶ Likelihood

$$\ln L(\boldsymbol{\theta}; \mathbf{d}) \propto [\mathbf{d} - \mathbf{m}(\boldsymbol{\theta})]^\top \boldsymbol{\Sigma}^{-1} [\mathbf{d} - \mathbf{m}(\boldsymbol{\theta})]$$

- ▶ Model

$$m_\ell^{ij}(\boldsymbol{\theta}) = b\sigma_8^i b\sigma_8^j C_{ij,\ell}^{\delta\delta} + f\sigma_8^i f\sigma_8^j C_{ij,\ell}^{VV} + b\sigma_8^i f\sigma_8^j C_{ij,\ell}^{\delta V} + b\sigma_8^j f\sigma_8^i C_{ji,\ell}^{\delta V}$$

- ▶ Parameters

$$\boldsymbol{\theta} = \{b\sigma_8^i\} \cup \{f\sigma_8^i\}$$

- ▶ Covariance

$$\Sigma_{\ell\ell'}^{ij,nk} = \frac{C_\ell^{in} C_\ell^{jk} + C_\ell^{ik} C_\ell^{jn}}{(2\ell + 1)\Delta\ell f_{\text{sky}}} \delta_{\ell\ell'}^K$$

Pipeline test I

$$m_{\ell}^i(\boldsymbol{\theta}) = b\sigma_8^i b\sigma_8^i C_{ii,\ell}^{\delta\delta} + f\sigma_8^i f\sigma_8^i C_{ii,\ell}^{VV} + 2b\sigma_8^i f\sigma_8^i C_{ii,\ell}^{\delta V}; \quad d_{\ell}^i = C_{\ell}^{HHI, Th}$$

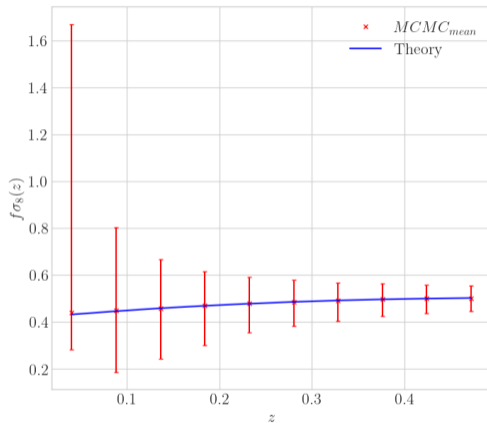
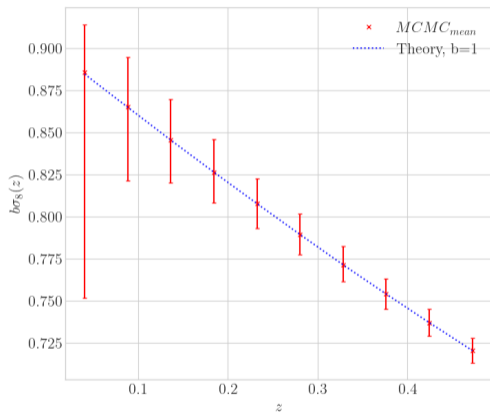
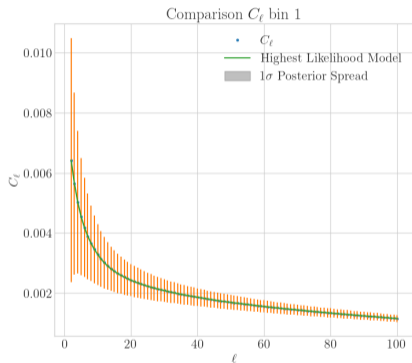


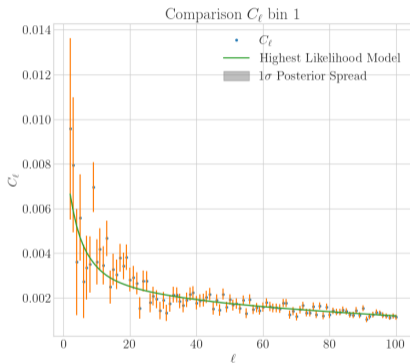
Figure: Estimation of artificial parameters

Pipeline test II

$$C_\ell \sim \mathcal{N}(C_\ell, \Sigma_\ell)$$



(a) Template



(b) Gaussian scattered data

Pipeline test III

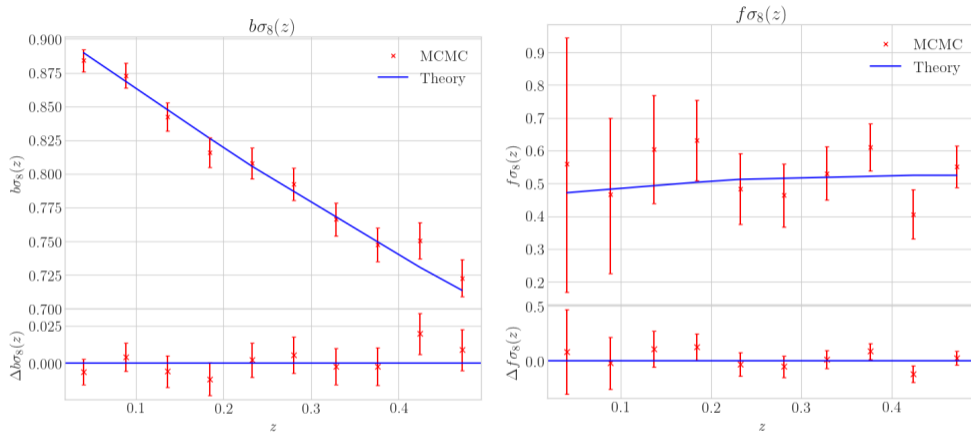


Figure: Estimation of artificial parameters

Intensity map

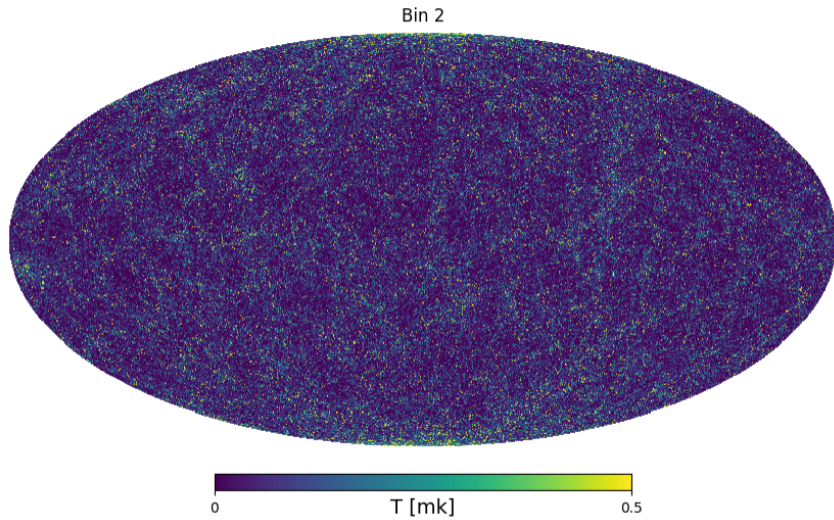


Figure: Intensity map at $z = 0.424$

$b\sigma_8$ and $f\sigma_8$ measure

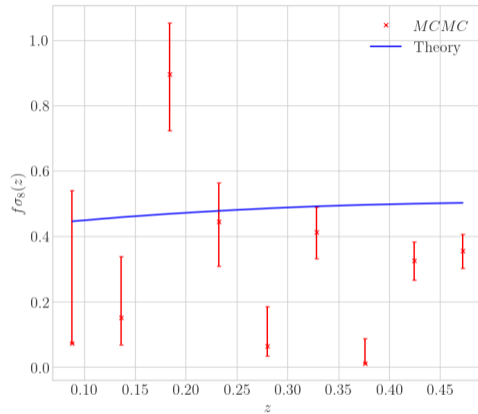
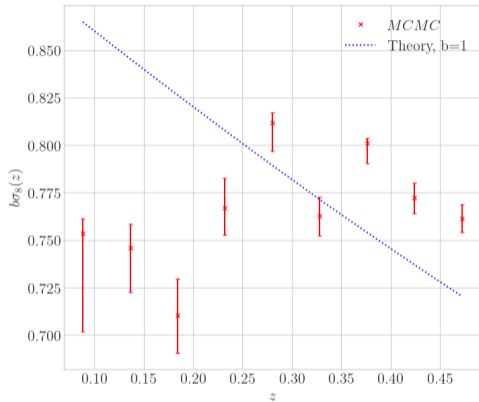


Figure: Estimation of maps parameters

Data

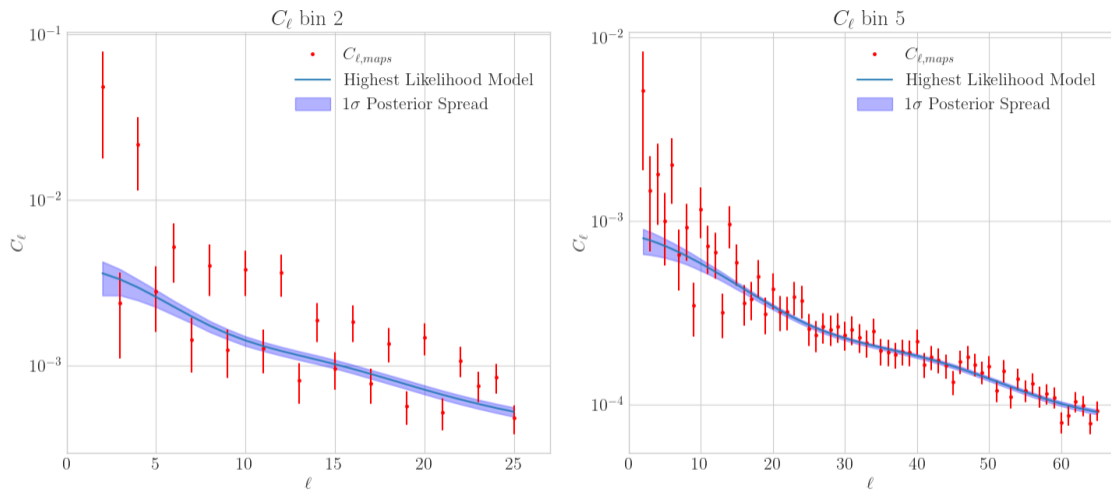


Figure: Data of bin 2 and 5

Shot Noise

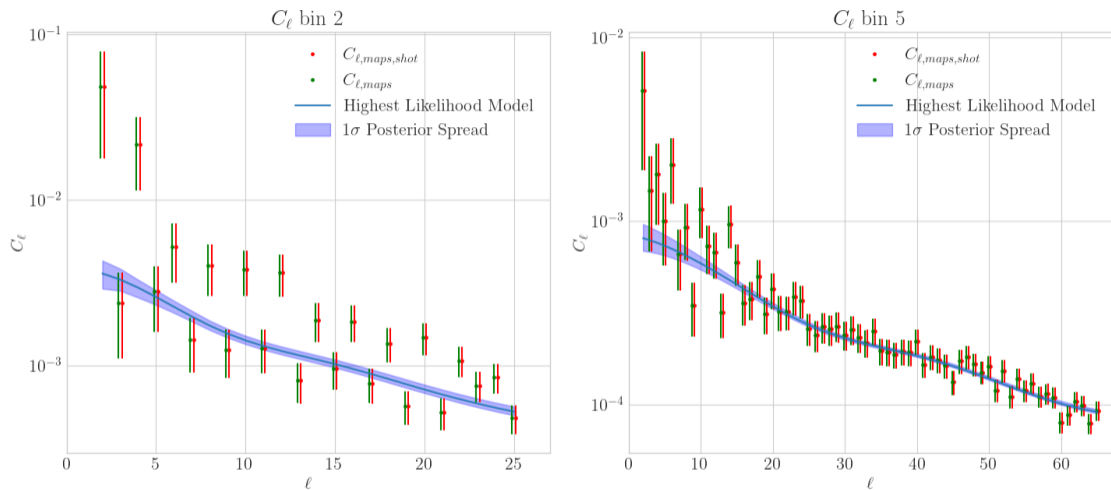


Figure: Data of bin 2 and 5

Noise as a free parameter

$$\Sigma_{\ell\ell'}^{ii} = \frac{2(C_\ell^{ii} + N^{ii})^2}{(2\ell+1)\Delta\ell f_{\text{sky}}} \delta_{\ell\ell'}^K$$

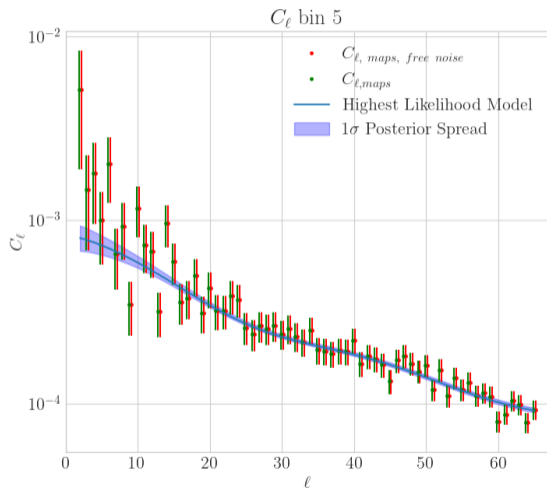
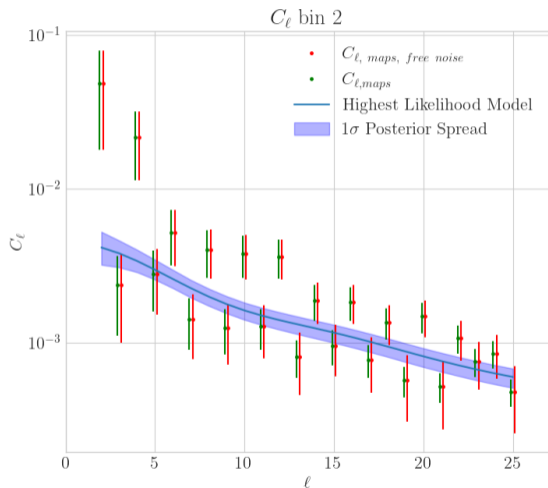


Figure: Data with noise of bin 2 and 5

Noise as a free parameter - Results

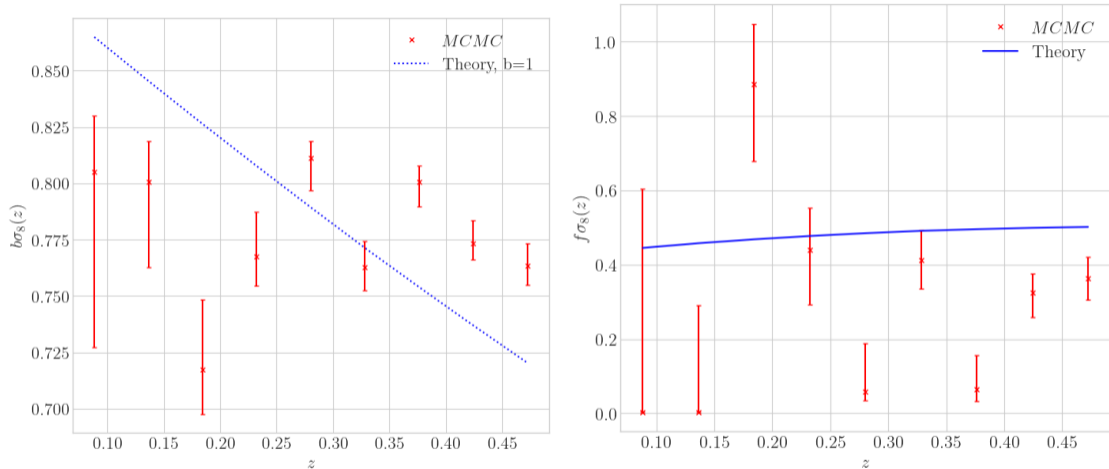
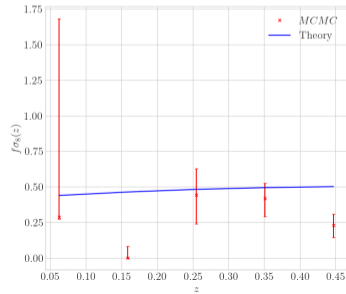
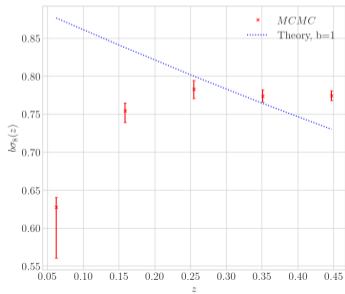
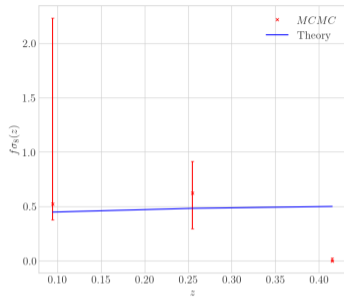
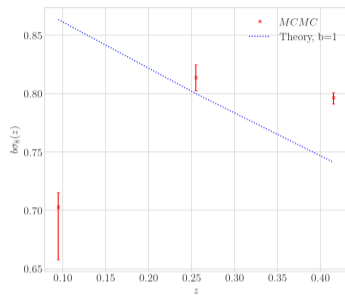


Figure: Estimation of parameters with noise

Other binning I



Other binning II

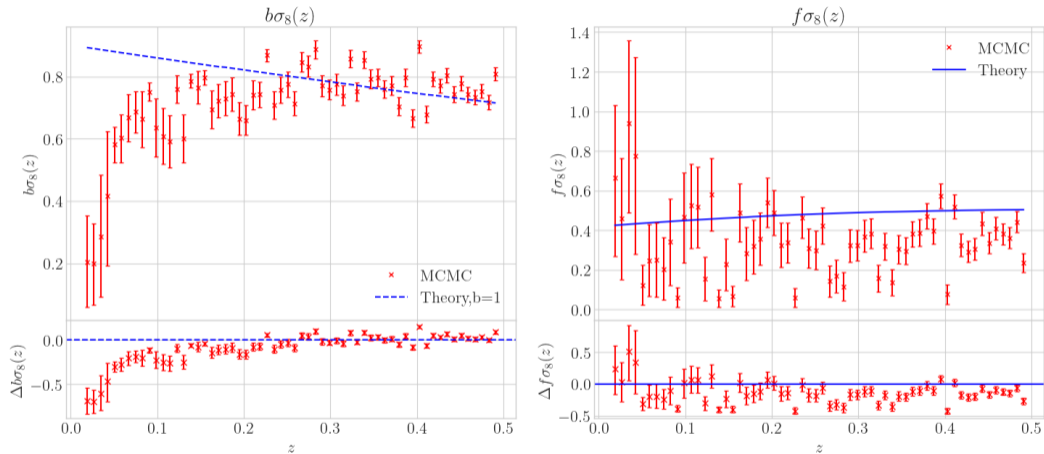


Figure: Estimation of parameters, 60 bins

Next steps

Template

Next steps

Template



Pipeline validation

Next steps

Template



Pipeline validation



Attempts of measuring $b\sigma_8$ and $f\sigma_8$

Next steps

Template



Pipeline validation

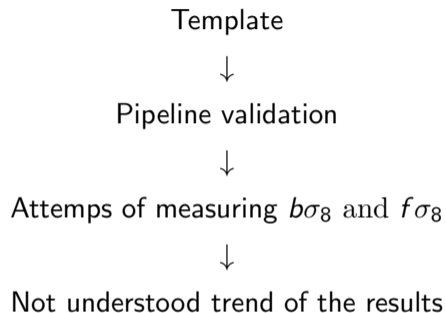


Attempts of measuring $b\sigma_8$ and $f\sigma_8$



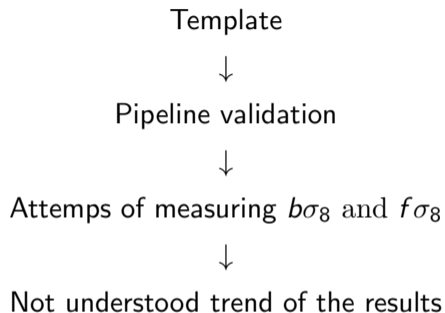
Not understood trend of the results

Next steps



- ▶ The **technique** behaviour is **validated**
- ▶ The work is continuing

Next steps



- ▶ The **technique** behaviour is **validated**
- ▶ The work is continuing



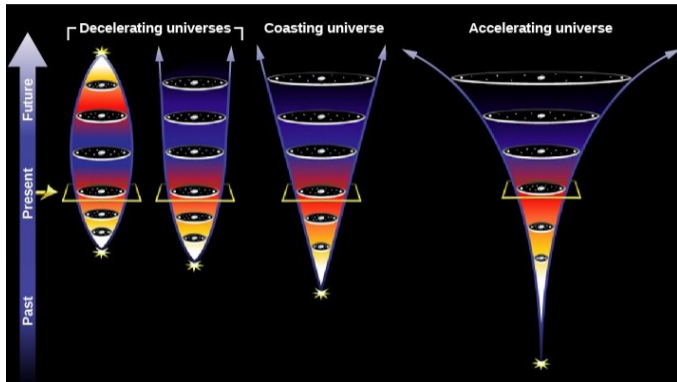
Rendering IM a reliable tool to provide new fresh data

Thanks for the attention!

Backup slides

Λ CDM Model

$$\Omega_b, \Omega_{\text{CDM}}, H_0, A_s, n_s, \tau$$



$$\Omega_k = 0 \quad \Omega_{\text{CDM}} \simeq 27\% \quad \Omega_\Lambda \simeq 70\%$$

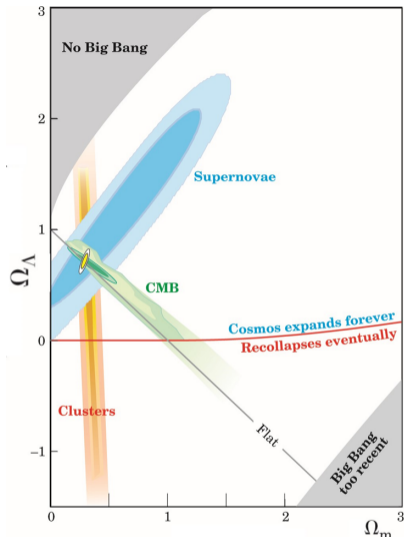


Figure: Cosmological parameters constraints [2–4]

Structures

$$\delta(\mathbf{r}) = \frac{\rho(\mathbf{r}) - \bar{\rho}}{\bar{\rho}}$$

Using $\mathbf{r} = \mathbf{r}(z)$, where $\mathbf{r} = r\hat{\mathbf{r}}$. In general

$$\delta(t) = D(t)\delta_i$$

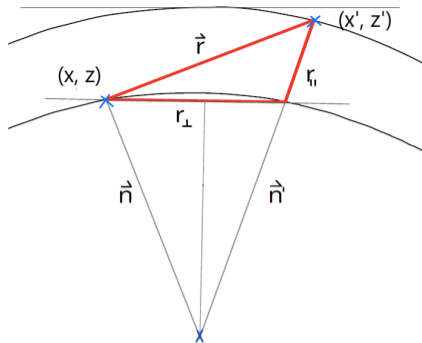
Gaussian distribution

$$\langle \delta(\mathbf{r}), \delta(\mathbf{r}') \rangle \equiv \xi(|\mathbf{r} - \mathbf{r}'|)$$

Power spectrum

$$\langle \delta(\mathbf{k}), \delta(\mathbf{k}') \rangle = (2\pi)^3 \delta_D^3(\mathbf{k} - \mathbf{k}') P(k)$$

$$P_i(k) = A_s k^{-n_s}$$



Spherical harmonics decomposition

The observer sees the perturbation variable projected onto a sphere

$$\Delta(\mathbf{r}) = \sum_{\ell m} a_{\ell m}(z) Y_{\ell m}(\hat{\mathbf{r}}) \quad a_{\ell m}(z) = \int d^2 \hat{\mathbf{r}} Y_{\ell m}^*(\hat{\mathbf{r}}) \Delta(\mathbf{r})$$

Here $\mathbf{r} = \mathbf{r}(z)$, where $\mathbf{r} = r \hat{\mathbf{r}}$.

$$\langle \Delta(\mathbf{r}), \Delta(\mathbf{r}') \rangle = \sum_{\ell=0}^{\infty} C_{\ell}(z, z') \sum_{m=-\ell}^{\ell} Y_{\ell m}(\hat{\mathbf{r}}) Y_{\ell m}^*(\hat{\mathbf{r}}') \quad (2)$$

Using the definition of Fourier transform $\Delta(\mathbf{r}) = \frac{1}{(2\pi)^3} \int d^3 \mathbf{k} \Delta(\mathbf{k}) e^{i\mathbf{k} \cdot \mathbf{r}}$ in equation 2

$$= \frac{1}{(2\pi)^6} \int d^3 \mathbf{k} d^3 \mathbf{k}' \Delta(\mathbf{k}) e^{i\mathbf{k} \cdot \mathbf{r}} \Delta^*(\mathbf{k}') e^{-i\mathbf{k}' \cdot \mathbf{r}'}$$

We moreover make use of the plane-wave expansion

$$e^{i\mathbf{k} \cdot \mathbf{r}} = 4\pi \sum_{\ell=0}^{\infty} i^{\ell} j_{\ell}(k r) \sum_{m=-\ell}^{\ell} Y_{\ell m}(\hat{\mathbf{k}}) Y_{\ell m}^*(\hat{\mathbf{r}})$$

Using physical form of the perturbation variable [1]

$$\Delta(\mathbf{r}) = b(z)\delta(\hat{\mathbf{r}}) + \frac{1}{\mathcal{H}(z)}\partial_r(\mathbf{V}(\mathbf{r}) \cdot \hat{\mathbf{r}}) + \dots$$

$$\delta(\hat{\mathbf{r}}) = \frac{1}{(2\pi)^3} \int d^3\mathbf{k} \delta(\hat{\mathbf{k}}) e^{i\mathbf{k} \cdot \mathbf{r}} \quad \frac{\partial}{\partial r}(\mathbf{V}(\mathbf{r}) \cdot \hat{\mathbf{r}}) = \frac{1}{(2\pi)^3} \int d^3\mathbf{k} \frac{V(\mathbf{k})}{k} \frac{\partial^2}{\partial r^2} (e^{i\mathbf{k} \cdot \mathbf{r}})$$

Data are grouped in $i, j = 1, \dots, N_b$ redshift bins containing $n^i(z)dz$ source per steradian

$$\Delta^i(\hat{\mathbf{r}}) = \int_{z_-}^{z_+} dz n^i(z) \Delta(\mathbf{r})$$

$$C_{ij,\ell}^{gg} = b\sigma_8^i b\sigma_8^j C_{ij,\ell}^{\delta\delta} + f\sigma_8^i f\sigma_8^j C_{ij,\ell}^{VV} - 2b\sigma_8^i f\sigma_8^j C_{ij,\ell}^{\delta V}$$

$$b\sigma_8(z) := b(z)D(z)\sigma_8; \quad f\sigma_8(z) := \frac{dD(z)}{d \ln(1+z)}\sigma_8$$

Structures

Growth factor [5]

$$D(a) = \frac{5\Omega_m}{2} \frac{H(a)}{a} \int_0^a \frac{da'}{a'^3 H(a')}$$

Factorized C_ℓ expressions [6]

$$C_{ij,\ell}^{\delta\delta} = \frac{2}{\pi} \int dk dr dr' k^2 \frac{P_{lin}(k)}{\sigma_8^2} n^i(r) n^j(r') j_\ell(kr) j_\ell(kr'),$$

$$C_{ij,\ell}^{VV} = \frac{2}{\pi} \int dk dr dr' k^2 \frac{P_{lin}(k)}{\sigma_8^2} n^i(r) n^j(r') j_\ell''(kr) j_\ell''(kr'),$$

$$C_{ij,\ell}^{\delta\delta} = \frac{2}{\pi} \int dk dr dr' k^2 \frac{P_{lin}(k)}{\sigma_8^2} n^{(i}(r) n^{j)}(r') j_\ell(kr) j_\ell''(kr').$$

Redshift and distances

$$d_c = \int_{t_e}^{t_0} c \frac{dt}{a(t)} \quad d = a(t)d_c$$

$$H(z) \equiv \frac{da}{dt} \frac{1}{a} = \frac{da}{dz} \frac{dz}{dt} (1+z); \quad da = -\frac{dz}{(1+z)^2}$$

$$dt = -\frac{dz}{(1+z)}$$

using Friedman equation

$$d_c = \frac{c}{H_0} \int_0^z \frac{dz'}{\sqrt{\Omega_r(1+z)^4 + \Omega_m(1+z)^3 + \Omega_k(1+z)^2 + \Omega_\Lambda}}$$

Brightness temperature

Given the Planck function for a black body

$$I_\nu = \frac{2h\nu^3}{c^2} \frac{1}{e^{\frac{h\nu}{kT}} - 1} \quad \left[\frac{W}{m^2 s^{-1}} \right]$$

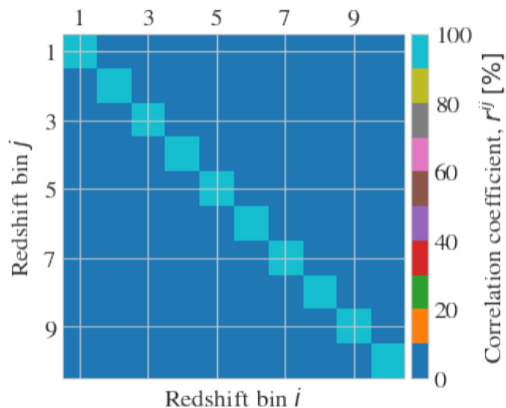
in the limit $h\nu \ll kT$ one can invert the relation obtaining

$$T_b = \frac{I_\nu c^2}{2k\nu^2}$$

Evaluating the cross correlations

Correlation coefficient

$$r^{ij} = \frac{\sum_{\ell} N_{\ell} \frac{C_{\ell}^{ij}}{\sqrt{C_{\ell}^{ii} C_{\ell}^{jj}}}}{N_{\ell}}$$



Shot noise

$$C_{\ell}^{shot} = T_{HI}^2(z)/\bar{N}(z), \quad (3)$$

$$\bar{N}(z) = n_0 c \int \frac{r^2(z)}{H(z)} dz. \quad (4)$$

Comoving number density of sources $n_0 = 0.03h^3 Mpc^{-3}$

i	1	2	3	4	5	6	7	8	9	10
$C_{\ell,min}^{ii}$	1.7×10^{-3}	4.8×10^{-4}	1.7×10^{-4}	1.1×10^{-4}	7.9×10^{-5}	6.5×10^{-5}	4.7×10^{-5}	3.7×10^{-5}	3.0×10^{-5}	2.6×10^{-5}
$C_{\ell}^{shot,ii}$	1.3×10^{-5}	3.4×10^{-6}	1.5×10^{-6}	8.9×10^{-7}	5.9×10^{-7}	4.3×10^{-7}	3.3×10^{-7}	2.7×10^{-7}	2.2×10^{-7}	1.9×10^{-7}

Covariance

$$\begin{aligned}
 \Sigma_{\ell\ell'}^{ij,nk} &= \text{Cov}(C_{\ell}^{ij}, C_{\ell'}^{nk}) \\
 &= \langle C_{\ell}^{ij} C_{\ell'}^{nk} \rangle - \langle C_{\ell}^{ij} \rangle \langle C_{\ell'}^{nk} \rangle \\
 &= \langle a_{\ell m}^i a_{\ell m}^j a_{\ell' m'}^n a_{\ell' m'}^k \rangle - C_{\ell}^{ij} C_{\ell'}^{nk} \\
 &= \langle a_{\ell m}^i a_{\ell m}^j \rangle \langle a_{\ell' m'}^n a_{\ell' m'}^k \rangle + \langle a_{\ell m}^i a_{\ell' m'}^n \rangle \langle a_{\ell m}^j a_{\ell' m'}^k \rangle + \\
 &\quad \langle a_{\ell m}^i a_{\ell' m'}^k \rangle \langle a_{\ell' m'}^n a_{\ell m}^j \rangle + C_{\ell}^{ij} C_{\ell'}^{nk} + o(a^3) \\
 &= C_{\ell}^{ij} C_{\ell'}^{nk} + C_{\ell}^{in} C_{\ell'}^{jk} \delta_{\ell\ell'}^K \delta_{mm'}^K + C_{\ell}^{ik} C_{\ell'}^{nj} \delta_{\ell\ell'}^K \delta_{mm'}^K - C_{\ell}^{ij} C_{\ell'}^{nk} \\
 &= \frac{C_{\ell}^{in} C_{\ell}^{jk} + C_{\ell}^{ik} C_{\ell}^{jn}}{(2\ell + 1)} \delta_{\ell\ell'}^K
 \end{aligned} \tag{5}$$

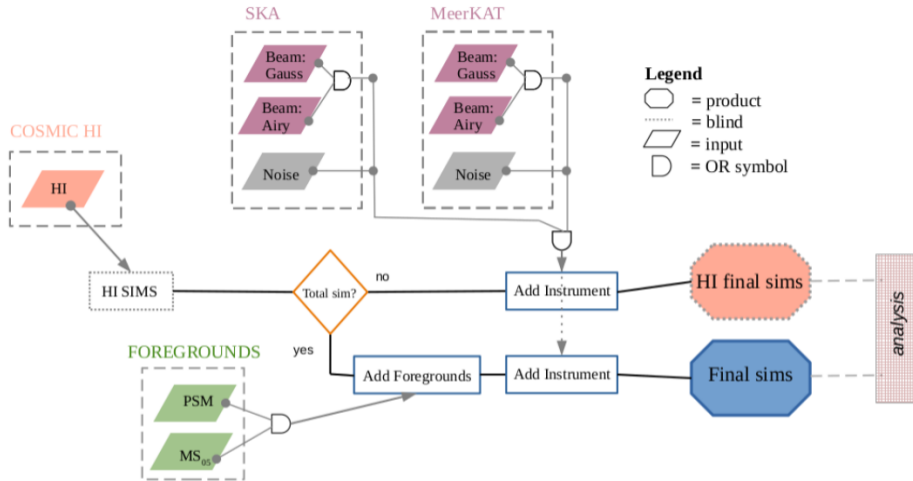


Figure: Foreground modelling and instrumental effects simulation. [7]

Other binning III

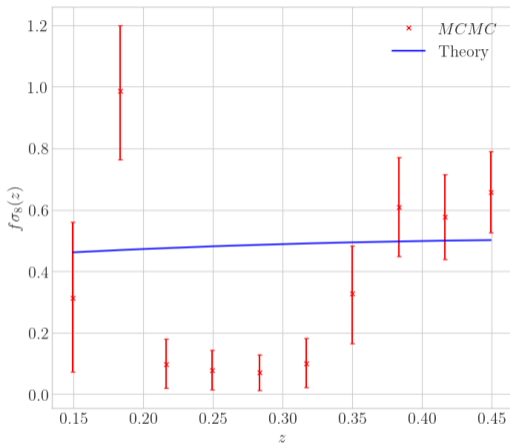
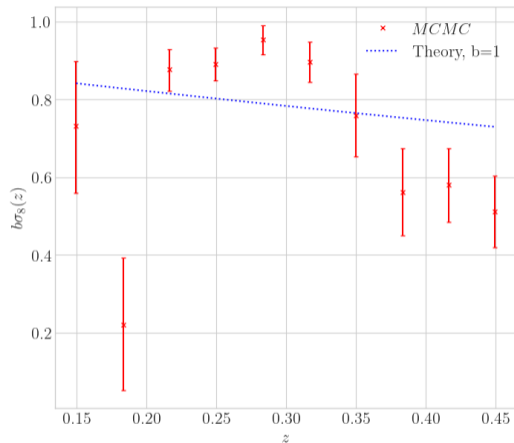


Figure: Estimation of parameters, 10 of the 512 original bins

References I

- [1] Camille Bonvin and Ruth Durrer. “What galaxy surveys really measure”. In: *Phys. Rev. D* 84 (6 Sept. 2011), p. 063505. DOI: [10.1103/PhysRevD.84.063505](https://doi.org/10.1103/PhysRevD.84.063505). URL: <https://link.aps.org/doi/10.1103/PhysRevD.84.063505>.
- [2] R. A. Knop et al. “New Constraints on Ω_m , Ω_Λ , and w from an Independent Set of 11 High-Redshift Supernovae Observed with the Hubble Space Telescope”. In: *The Astrophysical Journal* 598.1 (Sept. 2003), pp. 102–137. ISSN: 1538-4357. DOI: [10.1086/378560](https://doi.org/10.1086/378560). URL: <http://dx.doi.org/10.1086/378560>.
- [3] D. N. Spergel et al. “First-Year Wilkinson Microwave Anisotropy Probe (WMAP) Observations: Determination of Cosmological Parameters”. In: *The Astrophysical Journal Supplement Series* 148.1 (Sept. 2003), pp. 175–194. ISSN: 1538-4365. DOI: [10.1086/377226](https://doi.org/10.1086/377226). URL: <http://dx.doi.org/10.1086/377226>.

References II

- [4] S. W. Allen et al. “Cosmological constraints from the local X-ray luminosity function of the most X-ray-luminous galaxy clusters”. In: *Monthly Notices of the Royal Astronomical Society* 342.1 (June 2003), pp. 287–298. ISSN: 1365-2966. DOI: [10.1046/j.1365-8711.2003.06550.x](https://doi.org/10.1046/j.1365-8711.2003.06550.x). URL: <http://dx.doi.org/10.1046/j.1365-8711.2003.06550.x>.
- [5] D. J. Heath. “The growth of density perturbations in zero pressure Friedmann-Lemaitre universes.”. In: *MNRAS* 179 (May 1977), pp. 351–358. DOI: [10.1093/mnras/179.3.351](https://doi.org/10.1093/mnras/179.3.351).
- [6] Konstantinos Tanidis and Stefano Camera. *Model-independent constraints on clustering and growth of cosmic structures from BOSS DR12 galaxies in harmonic space*. 2021. arXiv: 2107.00026 [astro-ph.CO].

References III

- [7] M. Spinelli et al. “SKAO HI intensity mapping: blind foreground subtraction challenge”. In: *Monthly Notices of the Royal Astronomical Society* 509.2 (Oct. 2021), pp. 2048–2074. ISSN: 1365-2966. DOI: 10.1093/mnras/stab3064. URL: <http://dx.doi.org/10.1093/mnras/stab3064>.